JOURNAL OF Materials CHEMISTRY

New polyaniline–MoO_3 nanocomposite as a result of direct polymer intercalation

Oleg Yu. Posudievsky,* Svetlana A. Biskulova and Vitaly D. Pokhodenko

L. V. Pisarzhevsky Institute of Physical Chemistry of the National Academy of Sciences of the Ukraine, prospekt Nauki 31, Kiev 03039, Ukraine. E-mail: instphch@ukrtel.com; Fax: 38 044 265 62 16; Tel: 38 044 265 75 77

Received 3rd September 2001, Accepted 1st February 2001
First published as an Advance Article on the web 20th March 2002

A new nanocomposite based on polyaniline and MoO_3 is prepared *via* direct intercalation of conducting polymer macromolecules. The method of preparation allows material to be obtained with peculiar electric and electronic properties.

Introduction

Nanocomposites based on conducting polymers (CP) and transition metal oxides have been intensively investigated during recent years due to their potential for use as active components in electrode material in lithium batteries[1,2] and also as other optoelectronic devices.[3,4] These materials can be divided into two different types. The composites of the first type are prepared by polymerization of the appropriate monomers in the presence of an oxide dispersion, so the latter appear embedded in CP matrices, which frequently serves simultaneously as both conductor and binder.[1] The composites of the second type are guest–host compounds, when CP macromolecules are inserted into interlayer galleries or channels of inorganic particles.[2] Three methods of deriving such nanocomposites are known.[5] The first method includes the intercalation of monomers into the host matrix followed by their polymerization due to an external effect, for example, interaction with an oxidizer. In the second method, redox properties of the host ensure polymerization as well as intercalation of monomers *in situ*. The third method consists of direct intercalation of polymer macromolecules inside the host particles. Due to the large size of the macromolecules this is the most difficult to achieve. Meanwhile, its realization probably allows preparation of nanocomposites in which the macromolecules of the organic component will be inside channels of an inorganic component as in the nanocomposites prepared like that in, for example, ref. 2 as well as outside the inorganic particles as in the nanocomposites analogous to that described in ref. 1. In this case the nanocomposites contain structural elements characteristic of both types of nanocomposites and it seems feasible that they will be able to acquire the useful properties of both the analogs that have been mentioned. We think that this should be reflected, first of all, in the electrophysical and electrochemical properties and also in the character of the interactions between the organic and inorganic components of the nanocomposites.

In this paper, following such an approach an attempt has been made to prepare guest–host nanocomposites based on polyaniline doped with camphorsulfonic acid (PAn·CSA) and molybdenum oxide (MoO_3). Some physicochemical properties of the prepared material are also analyzed in comparison with the properties described in the literature for PAn·MoO_3 nanocomposites obtained by oxidative polymerization of intercalated anilinium using ammonium peroxydisulfate or iron chloride.[6,7]

Experimental

A solution of PAn·CSA in *m*-cresol was prepared according to the procedure specified in ref. 8. The emeraldine base utilized for the preparation of the nanocomposite was first purified of oligomers in a Soxhlet apparatus by acetonitrile and then purified of low molecular weight fractions of the polymer using successively tetrahydrofuran and dimethylformamide. The quantity of the dopant was chosen so that the doping level of the emeraldine base (assuming 50% oxidation) by monobasic acid was stoichiometrically equal to 50%. Aqueous 0.1% Li_xMoO_3 ($x = 0.41$) sol was prepared similarly to that described in ref. 9 by means of ultrasonic desintegration of lithiated molybdenum oxide for 1.5 hours and subsequent filtering. The sol was utilized in the synthesis of nanocomposites immediately after its preparation. Intercalation of lithium in MoO_3 (analytical grade), annealed previously in a muffle oven at 450 °C for 5 hours, was carried out *via* reaction of the oxide, thoroughly ground in an agate mortar, with a 1 M *n*-butyllithium solution in dry hexane in an argon atmosphere for 1 hour in a Schlenk flask with consequent vacuum drying at 70 °C for 3 hours. The content of lithium in Li_xMoO_3 was determined by measuring the decrease in concentration of *n*-butyllithium in the solution by titration with 0.1 M hydrochloric acid in the presence of phenolphthalein and by means of elemental analysis.

The content of metal in the materials was determined using atomic absorption spectroscopy. A Carlo Erba facility was used for C,H,N analysis. X-Ray powder diffractograms were obtained on a DRON 3M diffractometer using filtered Cu-K_α-irradiation; the accuracy of measured interatomic distances was 0.01 nm. IR spectra were registered on a UR-20 spectrometer on samples, as KBr pellets, with an accuracy of no less than 5 cm^{-1}. The EPR spectra were recorded on a Varian E-9 spectrometer utilizing a sample of Mn^{2+}, isomorphically substituted in the crystal lattice of MgO, as a standard for determining the *g*-factor and linewidth. The electrical conductivity was measured by means of the four-probe technique on pellets of the nanocomposite samples with an accuracy of about 10% with the ohmic character of the contacts with a conducting-polymer-based material being achieved by electrochemical deposition of gold on probe tips.

Results and discussion

The nanocomposite based on PAn·CSA and MoO_3 (PAn·CSA–MoO_3) was prepared by adding a *m*-cresol solution

 DOI: 10.1039/b107909c

of PAn·CSA to an aqueous sol of Li_xMoO_3 during mechanical stirring for 1 hour at room temperature. A dark green product was isolated by filtration and then washed with water and acetone. After drying in air, it was removed from the filter apparatus, ground in agate mortar and purified by extraction with acetonitrile in a Soxhlet apparatus, and then dried under vacuum at room temperature for 12 hours. The data from the elemental analysis testifies that the stoichiometry of the nanocomposite is $(PAn{\cdot}CSA_{0.124})_{1.06}MoO_3$ with a complete absence of lithium and with the content of *m*-cresol and water being equal to 4.2 and 9.5 wt% respectively.

It is necessary to mention that we have also carried out control experiments in which pure *m*-cresol or a solution of CSA in *m*-cresol were added to an aqueous sol of Li_xMoO_3, but that we did not detect any traces of intercalation of either solvent or acid molecules even after 24 hours.

The X-ray diffractogram of the prepared material contains two wide peaks with maximums at about 7.2° and 14.4° and one band of diffuse scattering with a maximum at about 26.5° (curve A in Fig. 1). The first two peaks correspond to interplanar spacings equal to 12.3 and 6.1 Å respectively. The shape of these peaks (corresponding to a high height to the half-width ratio) and also the presence in the spectrum of several (0*k*0) reflexes and the absence of (*hkl*) reflexes testify, in accord with results given in ref. 10 and 11, that the inorganic component of the composite possesses lamelar structure, the interlayer spacing in the particles being equal to 12.3 Å. The increase in the height of the interlayer galleries of 5.3 Å (from 7.0 Å in MoO_3 to 12.3 Å in the PAn·CSA–MoO_3 composite) agrees with intercalation of polyaniline macromolecules into MoO_3 particles with the phenyl rings located mainly perpendicular to theMoO_3 layers. In fact, it has been shown previously that for the PAn–V_2O_5 composite the increase in interlayer distance as a result of polymer intercalation amounts to 5.2–5.6 Å[10,12] and for PAn–$HMWO_6$ (M = Ta, Nb) nanocomposites the increase is equal to 5.35–5.4 Å.[13] From previous reports[10–13] it is believed that PAn chains occupy such positions in the galleries of the host. At the same time, for PAn–MoO_3 nanocomposites prepared as described in refs. 6 and 7 the increase in gallery height amounts to 6.7–6.8 Å, which, in the opinion of Nazar and co-workers,[7,14] is connected with the helical conformation of polymer macromolecules.

It should be noted that the arrangement of intercalated PAn macromolecules, presumably perpendicular to the layers of the inorganic component, established by us for PAn·CSA–MoO_3, is observed in all cases, when guest–host composites are prepared utilizing the method described in the present paper, *i.e. via* direct intercalation of doped PAn macromolecules from *m*-cresol solution into the galleries of inorganic nanoparticles.[15,16] This is apparently related to the influence of *m*-cresol, the solvent of PAn, which is also a secondary dopant, *i.e.* the substrate that promotes the stretched conformations of PAn chains.[17] Besides, the molecular weight of the intercalated polymer considerably exceeds that in the PAn–MoO_3 nanocomposites described in refs. 6 and 7.

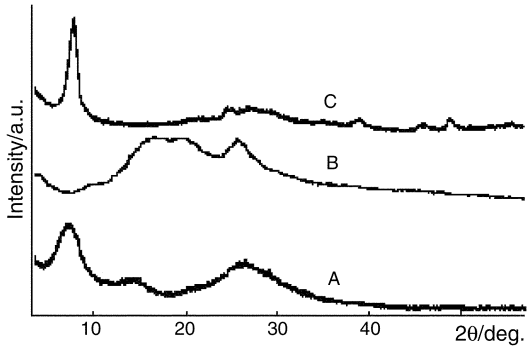

Fig. 1 X-Ray diffractograms of the PAn·CSA–MoO_3 nanocomposite (curve A), polymer PAn·CSA (curve B) and the Li_xMoO_3 bronze (curve C).

Comparison of the spectra presented in Fig. 1 allows us to conclude that the diffuse character of the band at about 26.5° is largely a result of the polymer component of the composite. The distance between adjacent macromolecules is equal to 3.4 Å which is the same as in the polymer PAn·CSA itself.[18] This fact testifies that the synthesis procedure has not significantly effected the compact arrangement of the chains observed in PAn·CSA. The polymeric macromolecules are inside interlayer galleries of inorganic particles, which form a structurally homogeneous phase of the composite, and, as on curve A, there are reflections that correspond to only one interlayer distance value.

The direct proof of the nanoscale size of the particles is the width of diffraction peaks, which is 2.8° and 1.0° for PAn·CSA–MoO_3 and Li_xMoO_3, respectively (curves A and C in Fig. 1). Then, the size (coherence length) of MoO_3 particles perpendicular to the layers, calculated according to Sherrer's equation,[19] is equal to 3 nm in the composite, which is approximately 3 times less than in the initial lithium bronze. The decrease in the coherence length of the nanocomposite in comparison with that of the parent xerogel, we believe, is a consequence of polymer chain insertion. During the preparation of the nanocomposite the part of the polymer chains which is outside the MoO_3 galleries, apparently, impedes the ordered precipitation of inorganic nanoparticles, as in the case of individual Li_xMoO_3. It is necessary to note that a similar decrease in crystallinity of the inorganic component is reported in ref. 12 for the PAn–V_2O_5 nanocomposite obtained *via* polymerisation and intercalation *in situ* (*via* the second of the methods described in the Introduction section). In contrast to this, Nazar and co-workers[7] and ourselves[19] have detected an invariance of inorganic particle size in PAn–MoO_3 and PAn–V_2O_5 composites. In ref. 7, this conclusion was based on the analysis of electronic micrographs. In ref. 19, we, as in the present work, have used Sherrer's equation. To explain the observed differences in the particle size, we would like to note that solubility of PAn in DMF (in ref. 19 PAn–V_2O_5 nanocomposite was prepared *via* direct intercalation of the polymer dissolved in DMF) is insignificant and is apparently due only to the low molecular weight fractions of PAn. From the significant differences in the value of the molecular weight and accordingly in the length of PAn chains, it can be assumed that the nanocomposite has another supramolecular structure, when there is only a small part of the polymer component outside the channels or galleries of inorganic nanoparticles or when there is none outside the inorganic nanoparticles. In this case the structure of the nanoparticles during precipitation of the nanocomposite and sol should result in similar sizes of crystalline areas, as is observed experimentally.

In the IR spectrum of the PAn·CSA–MoO_3 nanocomposite there are bands characteristic of both components.[19,20] The intensive band at about 1130 cm^{-1} (Fig. 2, curve A) is due to oscillations of B–N^+H=Q or B–N^+–B (B and Q are benzenoid and quinoid structures) fragments of doped PAn chains.[21] However, compared with the same band for the polymer PAn·CSA (Fig. 2, curve B), this band in the nanocomposite has a shoulder at about 1160 cm^{-1}. The presence of such an absorption is characteristic of the nondoped form of PAn. Therefore it is possible, apparently, to make a conclusion about the coexistence of doped and nondoped forms of PAn in the investigated nanocomposite owing to a lowering of the doping level of the polymer. Such a lowering is probably connected with the deintercalation of lithium during the synthesis of the nanocomposite.

Another feature of the IR spectrum is the position of the band corresponding to the oscillations due to Mo=O bonds. It shifts from 1000 to 960 and then to 945 cm^{-1} on transition from MoO_3 used for preparing the lithium bronze, to Li_xMoO_3

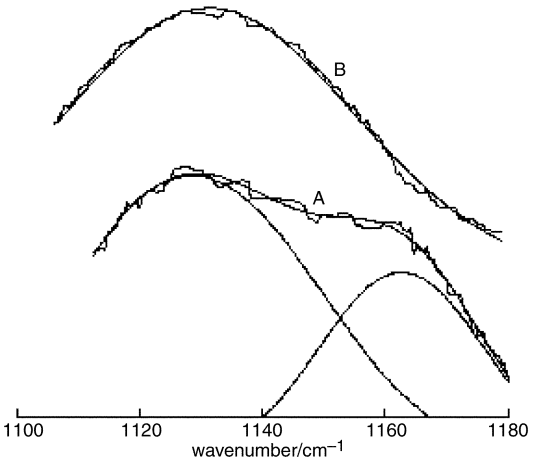

Fig. 2 IR spectra of the PAn·CSA–MoO_3 nanocomposite (curve A) and polymer PAn·CSA (curve B).

and then to the nanocomposite. This shift reflects the tendency for the interlayer distance to increase at first after intercalation of lithium and then after substitution of lithium by macromolecules of PAn. This is in accord with the tendency reported in ref. 22, where the red shift of the considered band during an increase in the degree of lithium intercalation (increase in interlayer distance) is marked. It is necessary to emphasize that the increase in the interlayer distance in Li_xMoO_3 as a result of lithiation is accompanied by an increase in the total negative charge of MoO_3 owing to its reduction. If we assume that the nature of the change of the band frequency in the PAn·CSA–MoO_3 nanocomposite is the same as in Li_xMoO_3, then it follows that the inorganic component in the nanocomposite is even more reduced than in the initial Li_xMoO_3 bronze. To test such an assumption we have studied the nanocomposite by means of EPR spectroscopy.

The EPR signal of the PAn·CSA–MoO_3 nanocomposite is represented by a singlet with $g = 2.0025 \pm 0.0003$ and linewidth $\Delta H_{pp} = 10.8 \pm 0.1$ G (Fig. 3). The value of the *g*-factor, which is similar to that of a free electron (Fig. 3, curve B), and also the absence from the spectrum of the signal with $g = 1.94$, which is characteristic of paramagnetic Mo^{5+} ions, that are present in the partially reduced MoO_3 layers of the Li_xMoO_3 bronze (Fig. 3, curve C), show that the signal is due to the paramagnetic centres of the polymeric component of the nanocomposite. A feature of the EPR spectrum is the absence of the signal due to ions Mo^{5+} that forces us to make the conclusion that MoO_3 in the prepared nanocomposite is not in the reduced state. This essentially distinguishes the PAn·CSA–MoO_3 nanocomposite obtained in the present work from its analogs reported in refs. 6 and 7 for which, as is noted by the authors, the presence of partially reduced molybdenum oxide is characteristic.

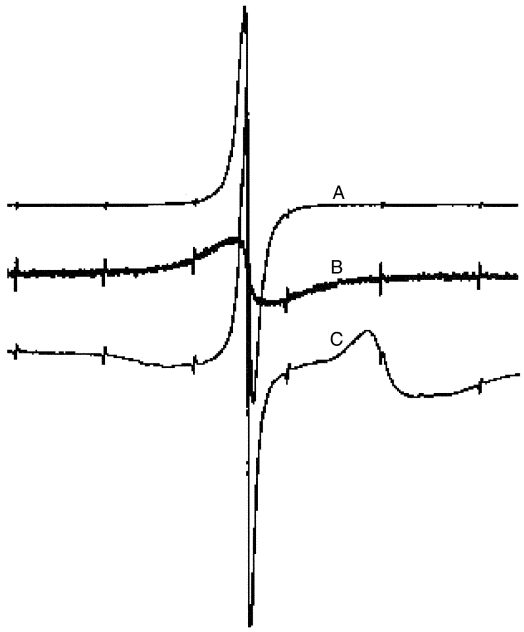

Fig. 3 EPR spectra of the PAn·CSA–MoO_3 nanocomposite (curve A), polymer PAn·CSA (curve B) and the Li_xMoO_3 bronze (curve C) on the background of Mn^{2+} as standard.

It should be emphasized that such a conclusion is in direct contrast to the assumption about the state of MoO_3 in the nanocomposite, which was made above on the basis of IR data concerning the behaviour of the band appropriate to Mo=O bond oscillations. According to ref. 22 mentioned above, the red shift of this band detected by us could be considered as a consequence of the increase in the interlayer spacing accompanying the reduction of MoO_3, whereas the data from EPR spectroscopy deny the presence in the nanocomposite of an appreciable quantity of Mo^{5+} paramagnetic ions formed as a result of reduction. After analysis of this conflict we do not consider it obligatory to link the decrease in vibrational frequency of the Mo=O bond, detected in the nanocomposite, with the reduction of MoO_3. Analogy with results given in ref. 22 is possible only in connection with the conclusion that the observed red shift is accompanied by an increase in the interlayer distance in MoO_3. We believe that during intercalation of doped (*i.e.* protonated) PAn chains inside galleries of MoO_3 nanoparticles the positively charged fragments of the polymer interact with reduced Mo^{5+} ions according to Scheme 1 with resulting dedoping of the polymer inside MoO_3 and a significant decrease in degree of its reduction. Within the framework of this model, the data of IR and EPR spectroscopies become mutually consistent because the EPR spectrum should not contain the signal of paramagnetic Mo^{5+} ions and the vibrational frequency of the Mo–OH bond is apparently less than that of the Mo=O bond, as is observed experimentally.

For examination of the validity of Scheme 1, we have dissolved Li_xMoO_3 and the PAn·CSA–MoO_3 nanocomposite in concentrated hydrochloric acid. The EPR spectra of the solutions obtained , presented in Fig. 4, practically coincide and contain a sextet of lines with $g_\perp = 1.949 \pm 0.001$ and $A_\perp = 50 \pm 2$ G (the longitudinal component of the g-tensor is not displayed in the spectrum at room temperature) characteristic for molybdenum ions in solution. Certainly, Fig. 4 provides the reason for analysis of the extent of proton localisation within the framework of Scheme 1, especially if one takes into account the data about the special nature of protons in PAn published recently,[23] so we consider this question the subject of a separate discussion.

The method used by us for the preparation of the nanocomposite also allows an essential increase in the electrical conductivity of the resulting material (Table 1). The observed increase in conductivity is stipulated by the large length of PAn chains and consequently by the presence of direct contact between the chains outside MoO_3 and also by secondary doping of the polymer with the initial solvent. Besides, in the PAn·CSA–MoO_3 nanocomposite there are no traps of charge carriers on the interface between the composite components, which are apparently present in the nanocomposites reported in refs. 6 and 7 because the conductivity of the polymer is

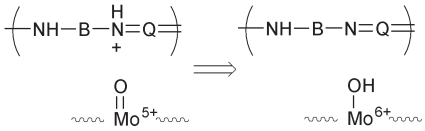

Scheme 1

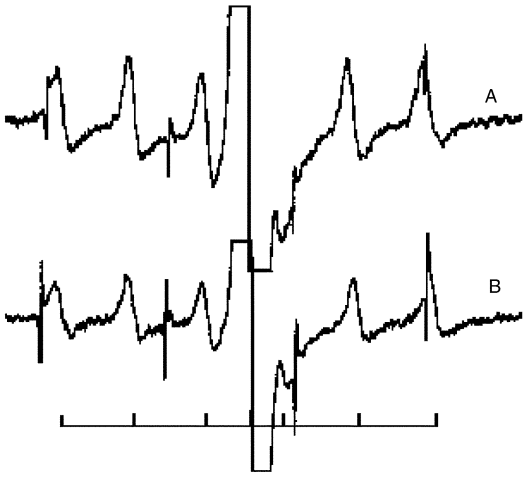

Fig. 4 EPR spectra of the PAn·CSA–MoO_3 nanocomposite (curve A) and Li_xMoO_3 bronze (curve B), dissolved in concentrated HCl, using Mn^{2+} standard.

p-type and that of reduced MoO_3 is n-type. It is interesting to note that the conductivity of PAn·CSA–MoO_3 is more than an order of magnitude less than that of the PAn·CSA–V_2O_5 nanocomposite prepared by us *via* a similar route.[15] We believe this may be related to differences in the procedures used for preparing the initial aqueous sols of the inorganic components. In the case of V_2O_5, the stable sol is obtained without preliminary lithiation of the oxide.[15] In the case of PAn·CSA–MoO_3, during preparation of the nanocomposite substitution of lithium and water in the interlayer galleries of the Li_xMoO_3 nanoparticles by macromolecules of PAn takes place. As a result of deintercalation of hydrated lithium ions, partial dedoping of PAn may take place. The data from the elemental analysis presented above confirm this assumption. In fact, according to the calculations carried out in ref. 7 on the basis of the length of the PAn molecular cell and the size of the basal cell of Li_xMoO_3, the upper limit of the theoretical stoichiometry of the nanocomposite, when the polymer is only inside oxide particles, amounts to $PAn_{0.33}MoO_3$. Here it is necessary to note that during intercalation of the polymer, CSA, which is not bound to PAn, is also formed. (This conclusion may be apparently made if the expansion of the interlayer galleries on intercalation of PAn macromolecules does not depend on the nature and size of the dopant and is determined by the size of phenyl ring of the polymer.[15,16,19]) As the degree of of dopint of the initial PAn·CSA was 50%, it means that after intercalation there are 0.165 mol of CSA (per 1 mol of MoO_3) outside the galleries of the inorganic host. This implies that as a result of displacement of 0.41 mol of lithium from the interlayer galleries of MoO_3 during synthesis, 0.245 mol of Li^+ can interact with PAn·CSA, which is outside of the MoO_3 galleries and dedope it. As outside the galleries of MoO_3 there are $1.06 - 0.33 = 0.73$ mol of PAn, the degree of doping of PAn in the nanocomposite should be equal to $0.73 - 0.5 - 0.245 = 0.120$ which is similar to the data from the elemental analysis.

Conclusion

Thus, some physicochemical features of the new guest–host nanocomposite based on PAn·CSA and MoO_3 are described in the present work. The fact that during synthesis there is substitution of lithium in nanoparticles of Li_xMoO_3 by PAn macromolecules dissolved in *m*-cresol, which poorly dissolves in water, in our opinion, should be in particular noted. The new route for preparation of the nanocomposite allows material with conductivity 2–3 orders greater than that of known analogs to be obtained. This, apparently, is basically a result of the secondary doping of PAn in the initial solution. The inorganic component of the nanocomposite is not in the reduced state.

Table 1 Conductivity of the nanocomposites based on PAn and MoO_3

	PAn·CSA–MoO_3	PAn–MoO_3[8]	PAn–MoO_3[9]
Conductivity/ S cm^{-1}	6.4×10^{-1}	3×10^{-3}	5×10^{-4}

Acknowledgement

The financial support of the Ministry of Education and Science of the Ukraine is gratefully acknowledged.

References

1 S. Kuwabata, S. Masui and H. Yoneyama, *Electrochim. Acta*, 1999, **44**, 4593.
2 G. R. Goward, F. Leroux and L. F. Nazar, *Electrochim. Acta*, 1998, **43**, 1307.
3 P. k. H. But, D. S. Thomas, R. H. Friend and N. Tessler, *Science*, 1999, **285**, 233.
4 F. Marlow, M. D. McGhee and D. Zhao, *Adv. Mater.*, 1999, **11**, 632.
5 Y.-J. Liu, D. C. DeGroot, J. L. Schindler, C. R. Kannerwurf and M. G. Kanatzidis, *Adv. Mater.*, 1993, **5**, 369.
6 R. Bissessur, D. C. DeGroot, M. G. Kanatzidis, J. L. Schindler and C. R. Kannewurf, *J. Chem. Soc., Chem. Commun.*, 1993, 687.
7 T. A. Kerr, H. Wu and L. F. Nazar, *Chem. Mater.*, 1996, **8**, 2005.
8 Y. Cao, P. Smith and A. J. Heeger, *Synth. Met.*, 1993, **57**, 3514.
9 J. P. Lemmon and M. M. Lemer, *Solid State Commun.*, 1995, **94**, 533.
10 M. G. Kanatzidis and C.-G. Wu, *J. Am. Chem. Soc.*, 1989, **111**, 4139.
11 M. G. Kanatzidis, C.-G. Wu, H. O. Marcy, D. C. DeGroot and C. R. Kannewurf, *Chem. Mater.*, 1990, **2**, 222.
12 M. Lira-Cantu and P. Gomez-Romero, *J. Electrochem. Soc.*, 1999, **146**, 2029.
13 B. E. Koene and L. F. Nazar, *Solid State Ionics*, 1996, **89**, 147.
14 G. R. Goward, T. A. Kerr, W. P. Power and L. F. Nazar, *Chem. Commun.*, 1998, 449.
15 V. D. Pokhodenko, Ya. I. Kurys, Yu. K. Malinovsky and O. Yu. Posudievsky, unpublished results.
16 V. D. Pokhodenko, Ya. I. Kurys, Yu. K. Malinovsky and O. Yu. Posudievsky, to be submitted.
17 G. MacDiarmid and A. J. Epstein, *Synth. Met.*, 1994, **65**, 103.
18 D. G. Minto and A. S. Vaughan, *Polymer*, 1997, **38**, 2683.
19 V. D. Pokhodenko, V. A. Krylov, Ya. I. Kurys and O. Yu. Posudievsky, *Phys. Chem. Chem. Phys.*, 1999, **1**, 905.
20 L. F. Nazar, H. Wu and W. P. Power, *J. Mater. Chem.*, 1995, **5**, 1985.
21 S.-A. Chen and L.-C. Lin, *Adv. Mater.*, 1995, **7**, 473.
22 N. Kumagai, N. Kumagai and K. Tanno, *J. Appl. Electrochem.*, 1988, **18**, 857.
23 F. Fillaux, *Solid State Ionics*, 1999, **125**, 69.